琉球大学学術リポジトリ

Adsorption of diatomic molecules on iron tape-porphyrin : A comparative study

メタデータ	言語: 出版者: 公開日: 2021-06-18 キーワード (Ja): キーワード (En): 作成者: Escaño Mary, Clare Sison メールアドレス: 所属:
URL	http://hdl.handle.net/20.500.12000/48585

Adsorption of diatomic molecules on iron tape-porphyrin: A comparative study

Tien Quang Nguyen, Mary Clare Sison Escaño, Nobuaki Shimoji, Hiroshi Nakanishi, and Hideaki Kasai*
Department of Precision Science & Technology and Applied Physics, Graduate School of Engineering, Osaka University, 2-1 Yamadaoka, Suita, Osaka 565-0871, Japan
(Received 23 January 2008; published 9 May 2008)

We investigated the adsorption of diatomic molecules, CO, NO, and O_2, denoted by *X*O on iron tape-porphyrin (FeTP) using first-principles calculations based on density functional theory. In this work, we present the structure and electronic properties of iron tape-porphyrin and its complexes with CO, NO, and O_2. The binding of such diatomic molecules to FeTP gave rise to significant changes on both the geometric structure and electronic properties of FeTP. We found that in all FeTP complexes with diatomic molecules, the Fe atom moves out of the porphyrin plane toward the adsorbed molecule. The energy of the iron-diatomic molecule bond increases in the order of Fe-O_2 (0.554 eV)$<$Fe-CO (1.225 eV)$<$Fe-NO (1.719 eV). At its stable position, the Fe-*X*-O angle increases in the order of Fe-C-O$>$Fe-N-O$>$Fe-O-O. The changes in geometric structure are in accordance with other density functional theory calculations and experimental results for porphyrin molecule. As regards the electronic properties, there appears an energy gap between the conduction band and valence band in CO-adsorbed and NO-adsorbed cases with a more pronounced energy gap in the former, while none was observed in the O_2-adsorbed case. We attribute these changes in electronic properties to the strong interaction involving the *d* orbitals of the Fe atom and the π^* orbitals of diatomic molecules. Specifically, for the CO and NO adsorbed on FeTP cases, the change in electronic properties is attributed to the strong hybridization of d_{xz} and d_{yz} orbitals of the Fe atom and π^* orbitals. For O_2 adsorbed on FeTP, the hybridization of the d_{z^2} orbital of the Fe atom and π^* orbitals plays the key role in O_2–iron tape-porphyrin interaction.

DOI: 10.1103/PhysRevB.77.195307 PACS number(s): 31.15.ae, 87.15.B−, 31.15.E−, 81.07.Nb

I. INTRODUCTION

Since the Aviram and Ratner's pioneering paper, suggesting that molecules could perform the functions of semiconductor electronics,[1] there have been ample demonstrations that molecules can function as wires, rectifiers, memories, and switches.[2] To date, plenty of organic functional molecules have been synthesized. Along with this, recent advances in the fabrication technique of substrates, including metal electrodes, make it possible to realize molecular electronic devices.

Among the various types of functional molecules, the molecular wires have been extensively investigated both theoretically and experimentally. Most of the molecular wires are oligomers, whose structural units are composed of a few building blocks, such as thiophene, ethynylene, porphyrin, and so on.[3] The porphyrin is one of the building blocks from which several types of differently conjugated porphyrin molecular wires have been prepared.[4] In particular, tape-shaped porphyrin molecules (or tape-porphyrin), where the adjacent building blocks (referred to as porphyrin macrocycles) are linked via three conjugating C-C bonds (see Fig. 1), have attracted much attention due to their extremely small highest occupied molecular orbital–lowest unoccupied molecular orbital (HOMO-LUMO) energy gaps.[4] Therefore, the tape-porphyrin molecules are expected to be useful as good conducting molecular wires. In fact, the porphyrin wires are considered to be useful as parts in molecular devices, but there have been very few studies dealing with the detailed electronic properties of these molecules and on the interaction between wires and other complexes. To date, only Zn tape-porphyrin has been synthesized so far.[5–7] However, it is well known that a porphyrin ring can coordinate with many metal atoms such as Fe, Ni, Pt, etc.,[8–10] more especially with Fe.

An iron porphyrin molecule is a large heterocycle organic ring of heme group in the hemoglobin complex. It not only plays a fundamental role in carrying O_2 in blood but it also interacts with CO and NO to form the basis of many biological processes. There have been some previous studies on the geometric structure and electronic structure of iron porphyrin and its complexes with diatomic molecules.[11,12] On the other hand, there have been many studies on applications of iron porphyrin as catalyst in polymer electrolyte fuel cells.[13–15,27,28] However, in these studies, the authors have focused only on the iron porphyrin molecule and its complexes with diatomic molecules. In order to fully understand porphyrin systems and to find out other applications of such porphyrin complexes, we think that it is necessary to extend the study on both the geometric and electronic structures of

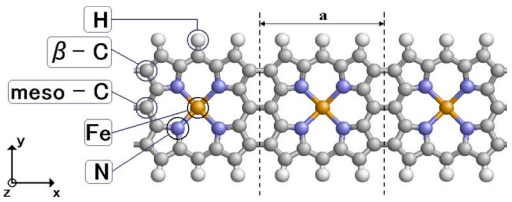

FIG. 1. (Color online) Top view of iron tape-porphyrin. The macrocycle unit, which links to others by three conjugating C-C bonds, is shown between two broken lines. The Fe atom is at the center of the macrocycle. Four atoms that connected to the Fe atom are N atoms. Hydrogen atoms lie on the edge of the tape along the *x*-axis direction.

 ©2008 The American Physical Society

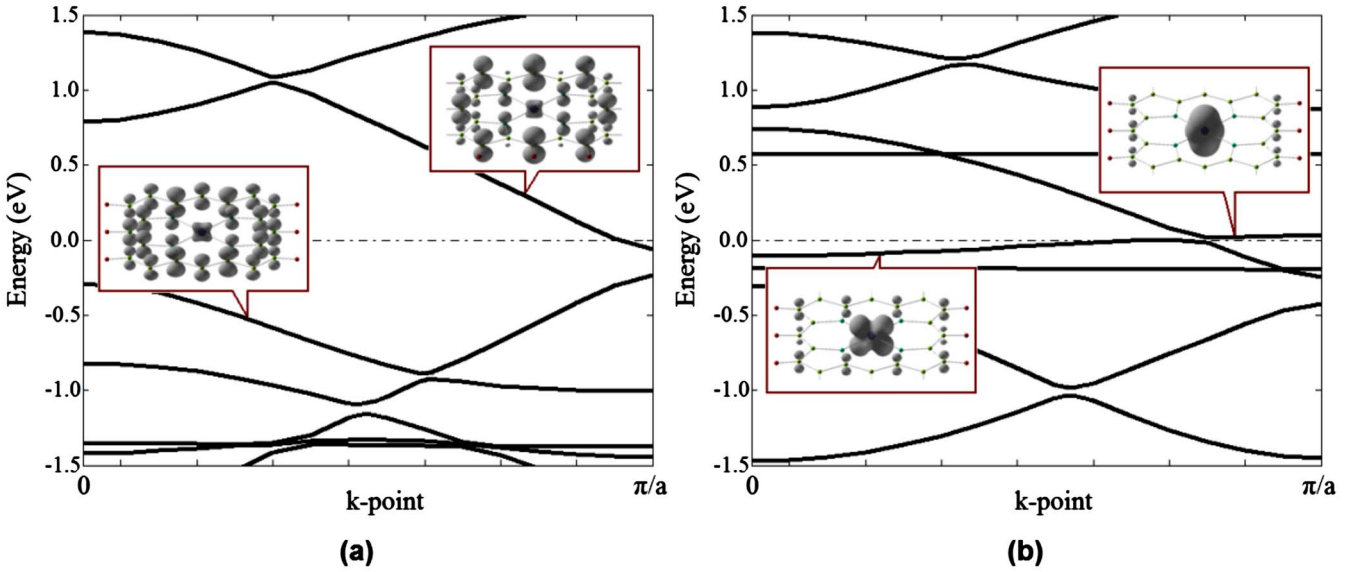

FIG. 2. (Color online) Band structures of (a) majority-spin and (b) minority-spin electrons for Fe tape-porphyrin. Isosurface plots denote the electron charge density distribution of the conduction band and valence band near the Fermi level. The Fermi level is set to origin. The charge density is displayed at 0.03 $e/\text{Å}^3$ isosurface value.

porphyrin complexes and conjugated porphyrin (sheet shape, T shape, tape shape, etc.) complexes. The interactions between the CO molecule and iron tape-porphyrin have been investigated by our group.[16] In that study, the electronic properties of iron porphyrin, iron tape-porphyrin, and its complex with CO were considered. In this present work, we show a detailed theoretical study on both the geometric structure and electronic properties of the iron tape-porphyrin and its complexes with CO, NO, and O_2. The comparison between three complexes (FeTP-NO, FeTP-CO, and FeTP-O_2) also are taken into account. Here, we discuss the optimized geometric structures, band structures, and changes in electronic structures of iron tape-porphyrin (FeTP) before and after binding to diatomic molecules.

II. CALCULATION METHOD

All calculations were performed within the density functional theory (DFT) framework by using the spin-polarized version of the Vienna *ab initio* simulation package (VASP).[17,18] Nonlocal correction in the form of the generalized gradient approximation[19] was included for the exchange-correlation function. The calculations used the projector augmented wave[20] potential to describe the electron-ion interaction. A grid of $30\times1\times1$ Monkhorst–Pack special k points is used,[21] which was found to sufficiently account for the Brillouin-zone integration. With such setting of k-point grid, we imply that the tape-porphyrin can be considered as a molecular wire. In order to avoid interactions between the tape-porphyrin in the cell with those in the neighboring cells, we introduce a vacuum region of about 8.00 Å for the y-axis and z-axis directions. Here, the tape lies along the x-axis direction, as shown in Fig. 1. The length of 8.00 Å is also the initial value for a cubic unit cell, which is used for relaxed calculations. In addition, full structure optimization was done by relaxing all atoms to within a force tolerance of 0.05 eV/Å. This was done first along with the electronic structure analyses of FeTP before the detailed investigation of diatomic molecules binding on FeTP was conducted. As a result, we determined an 8.36 Å cell length along the x axis. This value was used for later calculations to speed up the convergence. For partial electron charge density (or band decomposed charge density), we calculated charge distribution in some electronic bands that clearly show bonding and antibonding states of diatomic molecule and FeTP at Γ point in Brillouin zone. Since the partial charge density can be calculated from a preconverged wave function, therefore, we first ran a static calculation with full k points, as mentioned before for the system from which the partial charge density is determined. Then, the parameters to determine which particular band is considered and which k points to use are set.

III. RESULTS AND DISCUSSIONS

The electronic band structures of FeTP are shown in Figs. 2(a) and 2(b) for majority-spin and minority-spin electrons, respectively. It is clear that in the majority-spin electron band, the band line crosses the Fermi level, suggesting a metallic property of FeTP. This implies that FeTP can be considered for conducting molecular wire applications. Also in Figs. 2(a) and 2(b), the charge density distributions on the energy bands near the Fermi level are shown. We note a high dispersion on these bands, which is caused by the high charge density distribution on the d_{yz} orbital of the Fe atom and the p_z orbital of the *meso*-C and β-C atoms, more especially on *meso*-C atoms. The high charge density on the *meso*-C and β-C atoms also contributes to the formation of the bonds between the porphyrin macrocycles. By keeping most of the parameters and setting of the initial configuration for Fe spins in ferromagnetic and antiferromagnetic states,

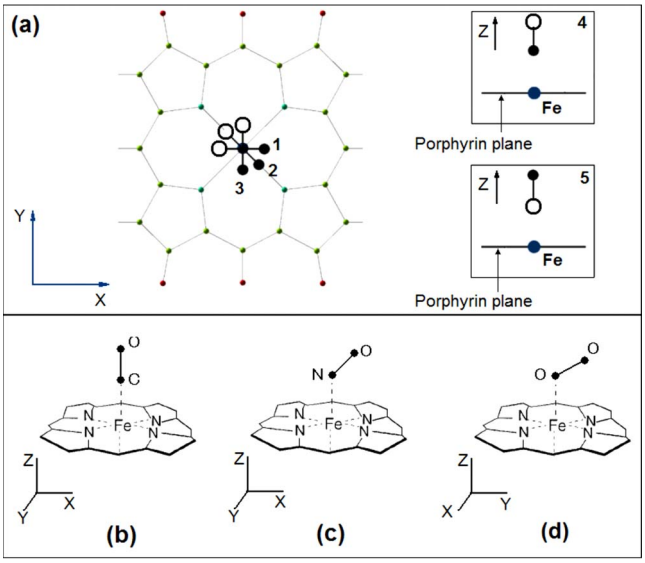

FIG. 3. (Color online) (a) Top view and side view of five initial adsorption sites of *X*O on FeTP and the structure for (b) CO-, (c) NO-, and (d) O_2-adsorbed Fe tape-porphyrin after relaxing.

we found that both resulted in a ferromagnetic state after relaxing the geometric structure. The total magnetic moment of the FeTP is $2.02\mu_B$ per one porphyrin macrocycle. The local magnetic moment of Fe atom per one unit cell is $2.12\mu_B$. This value is smaller than that of isolated Fe atom $(4\mu_B)$ because a part of this magnetization is canceled by the delocalization of the electron density in the tape-porphyrin structure. The calculations on the band structure and magnetic moment of tape-porphyrin are in good agreement with that of the previous study.[16] Also, the local magnetic moment of Fe atom changes upon adsorption of diatomic molecules. We found that the local magnetic moment of Fe atom is reduced, as compared to that of the Fe atom in FeTP $(2.12\mu_B)$. The Fe local magnetic moment is reduced to $0.87\mu_B$ and $0.90\mu_B$ in FeTP-NO and in FeTP-O_2, respectively. The Fe local magnetic moment in FeTP-CO, however, hardly changed, which may explain why its spin polarization disappeared.

Next, we discuss in detail the geometric structure and electronic structure of FeTP-*X*O. For the structure optimization of *X*O adsorbed on FeTP, we set some initial adsorption sites on top of FeTP, as shown in Fig. 3(a), to obtain the most

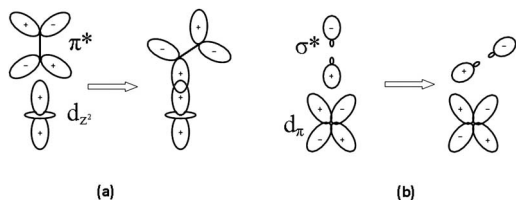

FIG. 4. The mechanism of forming the bent structure when the diatomic molecules bind to the iron tape-porphyrin. Here, d_π implies d_{xz} or d_{yz}. For the NO case, the first process $(d_{z^2}+\pi^*)$ is shown. However, in the case of O_2, both processes are included. This is the main factor that leads to the differences in the Fe-*X*-O angle.

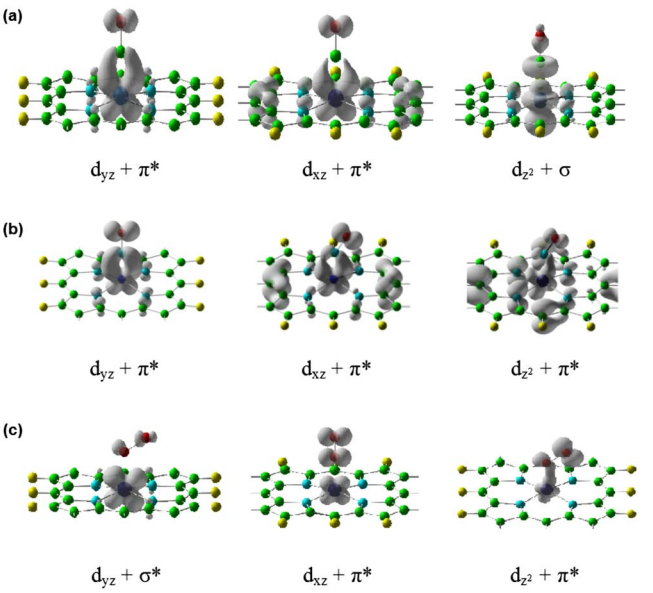

FIG. 5. (Color online) The partial (band decomposed) charge density at Γ point in the Brillouin zone of (a) FeTP-CO, (b) FeTP-NO, and (c) FeTP-O_2, which describe the hybridization between *d* orbitals and π^* orbitals. The charge density is displayed at 0.025 $e/\text{Å}^3$ isosurface value by VASP Data Viewer program.[26]

stable FeTP-*X*O geometric configuration. The optimized structures of FeTP-*X*O complexes in one unit cell after relaxing are described in Fig. 3(b). We found that the porphyrin macrocycles are domed in the space with ~0.2–0.3 Å deviation of Fe out of the porphyrin plane. The adsorption energies (E_{ads}) for three molecules relative to the iron tape-porphyrin and isolated gas molecule increase in the order of FeTP-O_2 (0.554 eV) < FeTP-CO (1.225 eV) < FeTP-NO (1.719 eV). This trend in binding is consistent with that reported in Ref. 11 for iron porphyrin using Car–

TABLE I. Comparison of the optimized structure of this work with some theoretical (DFT) and experimental results. Note that the complexes, which are investigated in these studies, are iron porphyrin molecules.

Structure		Fe-*X* (Å)	*X*-O (Å)	∡Fe-*X*-O
FeTP-CO	This work	1.70	1.17	180°
FeP-CO	DFT calc.[a]	1.69	1.17	180°
	Expt.[c]	1.77 ± 2	1.12 ± 2	179 ± 2°
FeTP-NO	This work	1.69	1.19	148°
FeP-NO	DFT calc.[a]	1.69	1.19	150°
	Expt.[d]	1.72 ± 1	1.12 ± 1	149 ± 1°
FeTP-O_2	This work	1.78	1.28	122°
FeP-O_2	DFT calc.[a]	1.74	1.28	123°
	Expt.[b]	1.75 ± 2	1.16 ± 4	131 ± 2°

[a]Reference 22.
[b]Reference 23.
[c]Reference 24.
[d]Reference 25.

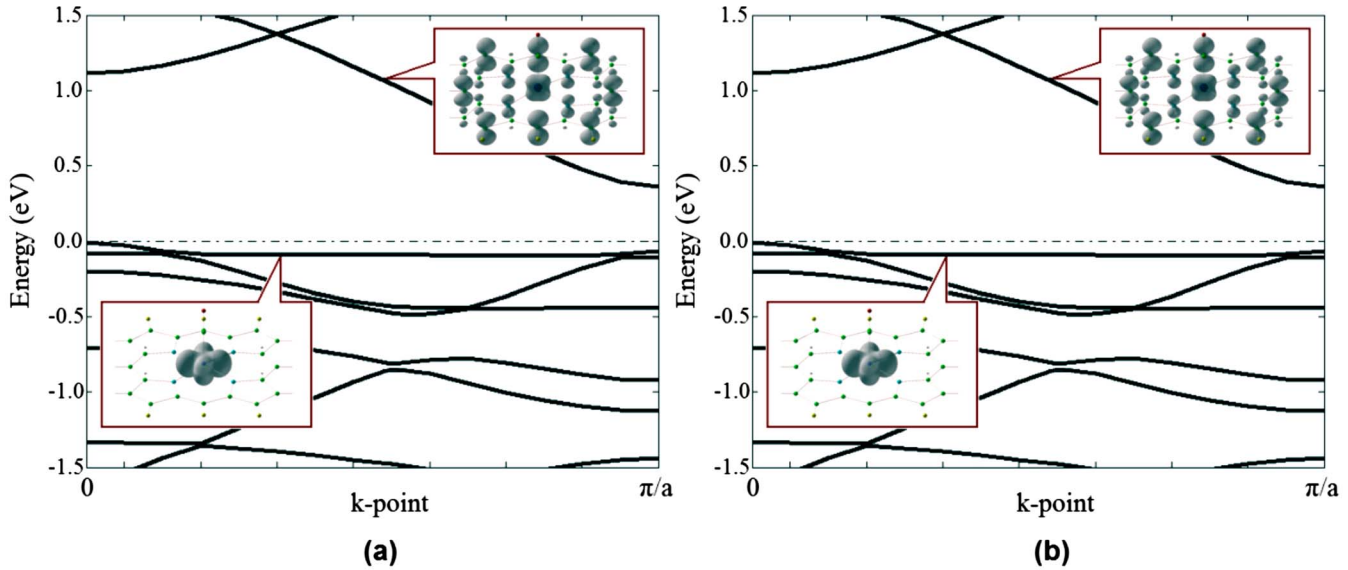

FIG. 6. (Color online) Band structure of (a) majority-spin and (b) minority-spin electrons for Fe tape-porphyrin with CO adsorbed. Isosurface plots denote the electron charge density distribution of the conduction band and valence band near the Fermi level. The Fermi level was set to origin. The charge density is displayed at 0.03 $e/\text{Å}^3$ isosurface value.

Parrinello molecular dynamics. The *X*-O bonds increase for all CO, NO, and O_2 cases, but the change in their bond lengths is minimal (0.03 Å for CO, 0.02 Å for NO, and 0.05 Å for O_2). Such stretches in bond lengths cannot break the *X*-O bonds. Therefore, it is difficult to dissociate *X*O molecules at the stable sites [here, we obtain end-on configuration for all structures, as shown in Figs. 3(b)–3(d)]. The direction of Fe-*X* bond is perpendicular to the porphyrin plane. The projections of *X*-O bonds lie along the bisector of N-Fe-N angle (nitrogen atoms of macrocycle). The Fe-*X*-O angle decreases in the order of Fe-C-O > Fe-N-O > Fe-O-O, the values of which are Fe-C-O = 180°, Fe-N-O = 148°, and Fe-O-O = 122°. This is taken to be due to the increase in nuclear charge from C to N to O, which lowers the π^* orbital energies of the *X*O molecules in the same order. Such differences in energy led to the differences in orbital hybridization of π^* orbitals of XO and *d* orbitals of Fe. For the FeTP-CO, the hybridization between the π^* orbital of CO molecule and d_{xz}, d_{yz} orbitals of Fe atom is noted. These interactions cause the linear structure of Fe-C-O. In addition, we also observe the hybridization between the d_{z2} orbital of Fe and the σ orbital of CO. However, we think that this kind of interaction does not deform the linear structure of Fe-C-O, as shown in terms of the partial charge density at Γ point in the Brillouin

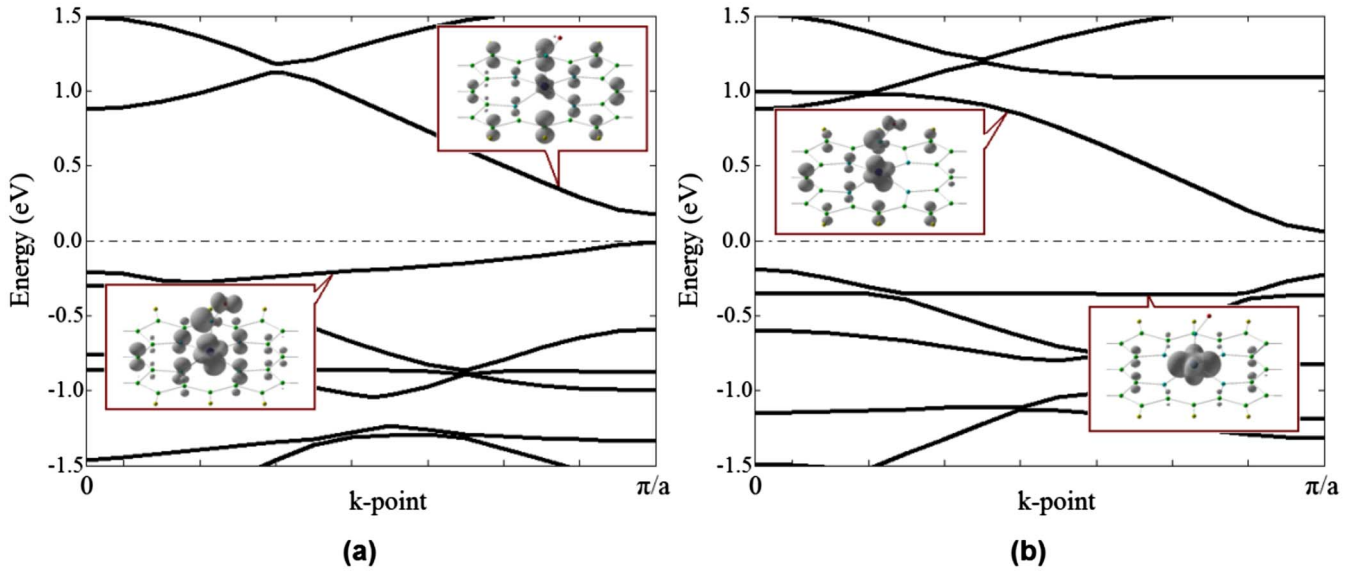

FIG. 7. (Color online) Band structures of (a) majority-spin and (b) minority-spin electrons for Fe tape-porphyrin with NO adsorbed. Isosurface plots denote the electron charge density distribution of the conduction band and valence band near the Fermi level. The Fermi level was set to origin. The charge density is displayed at 0.03 $e/\text{Å}^3$ isosurface value.

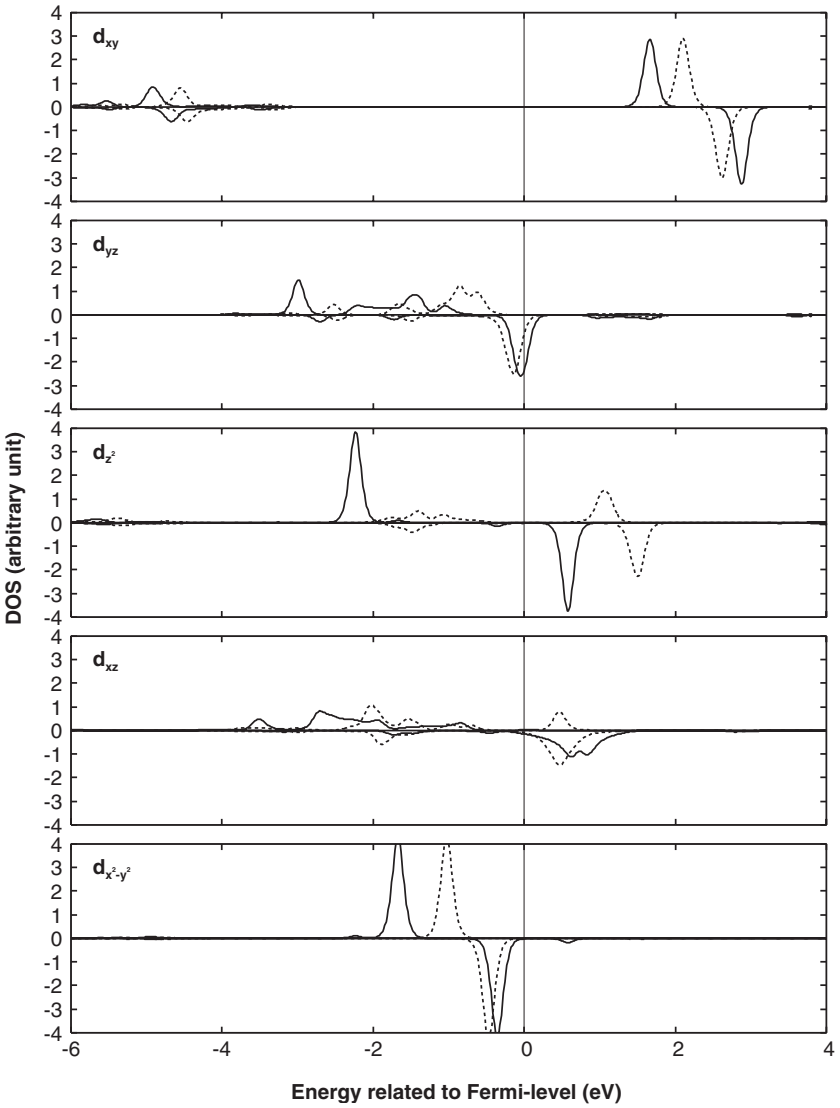

FIG. 8. The partial density of states of 3*d* orbitals of the Fe atom in FeTP (solid line) and FeTP-O_2 (dash line). In all subfigures, the unit for DOS is arbitrary and the unit for energy is eV. For each subfigure, the upper and the bottom panels correspond to spin-up and spin-down electrons, respectively. The Fermi level is shifted to zero.

zone on FeTP-CO in Fig. 5(a), where we can clearly see the partial charge density distribution on bonding orbitals of d_{xz}, d_{yz} with π^* and antibonding orbitals of d_{z^2} and σ. The hybridizations are completely symmetric following the z axis. Thus, it is difficult for CO to attain a bent structure. For FeTP-NO and FeTP-O_2, since the π^* orbitals are filled with one and two electrons, respectively, we expect a hybridization between π^* orbitals and the d_{z^2} orbital of Fe atom, which leads to a bent structure of Fe-N-O and Fe-O-O but with Fe-N-O angle (148°) greater than the Fe-O-O angle (122°). The differences in the bond angles can be explained in terms of the formation of bonding and antibonding between the σ^* orbital of O_2 molecule (LUMO) and the d_{yz} orbital of Fe atom. For NO adsorbed in the FeTP case, the HOMOs (π^* orbitals) are not completely filled. Therefore, such hybridization ($\sigma*$ with d) seems to be more difficult to occur for the NO adsorbed on FeTP than for the O_2 adsorbed on FeTP. The mechanism of these hybridizations is shown in Fig. 4. Here, we illustrated the interaction of the d_{z^2} with π^* and d_π with σ^* (d_π is denoted for d_{xz} and d_{yz} orbitals). For FeTP-NO, only the first process, which corresponds to the hybridization of the d_{z^2} orbital and π^* orbital, is included [Fig. 4(a)]. The results of orbital hybridization are shown in terms of the partial charge density at Γ point in the Brillouin zone in Figs. 5(b) and 5(c). In these figures, the charge density on d_{z^2} and π^* are clear. Also, the partial charge density distribution can be clearly seen on the bonding orbital of d_{xz} and π^* in the case of FeTP-NO, which we think significantly contributes to the greater Fe-N-O angle.

In Table I, we compare the results on the geometric structure of this work with some previous studies. The changes in geometric structure are in good agreement with other DFT calculations for porphyrin molecule[22] and with experimental results,[23–25] especially for FeTP-CO and FeTP-NO. For FeTP-O_2, our computational results for the O-O bond length and Fe-O-O angle are in good agreement with the DFT calculation[22] but at a little variance with the experimental results. The discrepancy might be due to the fact that the FeTP molecule (on which the experiments are based) contains four phenyl side groups. These phenyl groups interact with O_2 (van der Waals force) resulting to the difference between DFT calculations and experiment. Here, we emphasize that so far, no previous studies on the geometric structure for diatomic molecules adsorbed on iron tape-porphyrin were done. It is interesting to note, however, that the results

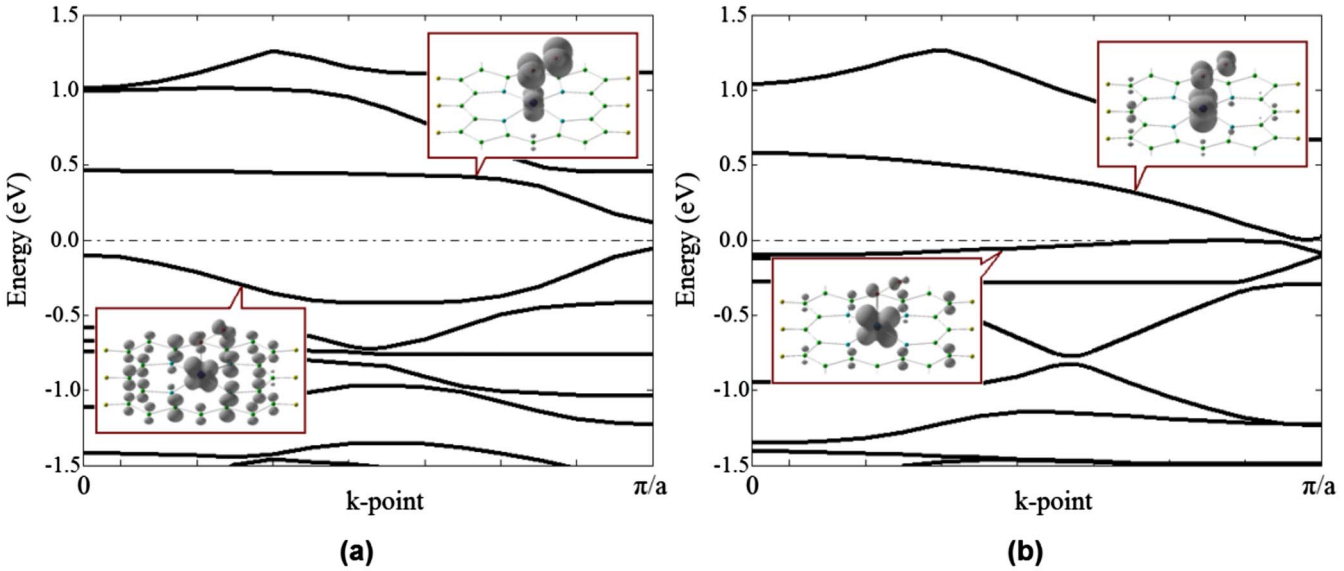

FIG. 9. (Color online) Band structures of (a) majority-spin and (b) minority-spin electrons for Fe tape-porphyrin with O_2 adsorbed. Isosurface plots denote the electron charge density distribution of the conduction band and valence band near the Fermi level. The Fermi level was set to origin. The charge density is displayed at 0.03 $e/\text{Å}^3$ isosurface value.

regarding the geometry of our work agree well with the DFT study on iron porphyrin in Ref. 22. We think that at the adsorption site, where diatomic molecules are directly on top of Fe atoms, the diatomic molecules insignificantly interact with one of the adjacent unit cells. Also, the bonds of *meso-meso*-carbon and β-β carbon do not induce considerable effects on diatomic molecules.

As mentioned previously, the iron tape-porphyrin has a conductive property, which is due to the high charge density distribution on p_z orbitals of *meso*-C atoms and on the d_{yz} orbital of the Fe atom. For the CO adsorbed on FeTP, a hybridization of the σ orbital of CO with the d_{z^2} orbital of Fe is observed, as well as a more effective π-back bonding (the hybridization of the d_π orbitals and π^* orbitals of CO),[16] as shown in Fig. 5(a). The d_{yz} and d_{xz} orbitals of the Fe atom, which correspond to the bands that cross the Fermi level in the case of FeTP, split into bonding and antibonding orbitals. This leads to an increase in the band energy gap between HOMO and LUMO, inducing the metal-insulator transition, as shown in Fig. 6. In the case of NO adsorbed on FeTP, we also get the transition from metallic to insulating because of the hybridization between d_{xz} and d_{yz} orbitals of the Fe atom and π^* orbitals of the NO molecule. However, the band energy gap in this case is small compared to that of CO adsorbed on FeTP. As previously discussed, because of the difference in molecular orbital energy, the π^* orbitals of NO molecule also hybridize with the d_{z^2} orbital of the Fe atom, and so we can see the charge density distribution of d_{z^2} orbital on the band energy near the Fermi level (Fig. 7). Moreover, the difference in orbital energy leads to the overlapping of π^* with d_{xz} and d_{yz}, which is somewhat different when compared to the CO-adsorbed case. These are taken to be the factors why we get a small energy gap in NO adsorbed on FeTP. We think that such argument above can also be applied for the last case, which is O_2 adsorbed on FeTP. As shown in Fig. 8, the DOS peak of d_{yz} and d_{xz} orbitals slightly changes. The main change is observed for the d_{z^2} orbital. As mentioned, the high charge density distribution on d_{yz} and d_{xz} orbitals is one of the factors that cause the metallic property of FeTP. Therefore, the binding of O_2 to FeTP does not drastically affect the electronic properties of FeTP. As illustrated in Fig. 9(b), no significant change in electronic properties of FeTP was observed when it coordinates with the O_2 molecule.

IV. CONCLUSIONS

In conclusion, we have used the DFT method to investigate structural and electronic properties of the iron tape-porphyrin and its interaction with CO, NO, and O_2. We found that the FeTP is metallic, and the adsorption of diatomic molecules on the FeTP induces significant changes in the geometric structure and the electronic properties of FeTP-*X*O complex. In the CO-adsorbed and NO-adsorbed cases, we note a metal-insulator transition; however, for the O_2-adsorbed case, no such change was observed. This is due to the difference in π^* orbital energies of diatomic molecules. In CO-adsorbed and NO-adsorbed cases, the electronic phase transitions are caused by the strong interaction between d_{xz} and d_{yz} orbitals of the Fe atom and π^* orbitals. In O_2 adsorbed on FeTP, the hybridization of d_{z^2} and π^* orbitals is considered as the main factor in the O_2-Fe interaction. The results of this work have shown potential in iron tape-porphyrin for molecular device applications—either as sensor or switch for detecting CO and NO.

ACKNOWLEDGMENTS

This work is supported by the Ministry of Education, Culture, Sports, Science and Technology of Japan (MEXT),

through their Grant-in-Aid for Scientific Research on Priority Areas "Development of New Quantum Simulators and Quantum Design" (No. 17064011) and Special Coordination Funds for the 21st Century Center of Excellence (COE) Program (G18) "Core Research and Advance Education Center for Materials Science and Nano-Engineering," Grants-in-Aid for Scientific Research (C) (19510108) programs. Some of the calculations were done using the computer facilities of the Cybermedia Center (Osaka University), the ISSP Super Computer Center (University of Tokyo), the Yukawa Institute (Kyoto University), and the Japan Atomic Energy Research Agency (JAEA).

*Corresponding author: kasai@dyn.ap.eng.osaka-u.ac.jp

[1] A. Aviram and M. A. Ratner, Chem. Phys. Lett. **29**, 277 (1974).
[2] C. Joachim, J. K. Gimzewski, and A. Aviram, Nature (London) **408**, 541 (2000).
[3] A. A. Farajian, R. V. Belosludov, H. Mezuseki, and Y. Kawazoe, Thin Solid Films **499**, 269 (2006).
[4] A. Tsuda and A. Osuka, Science **293**, 79 (2001).
[5] S. N. Song, D. M. Li, J. F. Wu, C. F. Zhuang, H. Ding, W. B. Song, L. F. Cui, G. Z. Cao, and G. F. Liu, Eur. J. Inorg. Chem. **2007**, 1844 (2007).
[6] M. Ptaszek, Z. Yao, D. Savithri, P. D. Boyle, and J. S. Lindsey, Tetrahedron **63**, 12629 (2007).
[7] D. Holten, D. F. Bocian, and J. S. Lindsey, Acc. Chem. Res. **35**, 57 (2002).
[8] J. P. Collman, Acc. Chem. Res. **10**, 265 (1977).
[9] M. Tsuda, E. S. Dy, and H. Kasai, Eur. Phys. J. D **38**, 139 (2006).
[10] M. S. Liao and S. Scheiner, J. Chem. Phys. **117**, 205 (2002).
[11] C. Rovira, K. Kunc, J. Hutter, P. Ballone, and M. Parrinello, Int. J. Quantum Chem. **69**, 31 (1998).
[12] H. Nakashima, J. Hasegawa, and H. Nakatsuji, J. Comput. Chem. **27**, 426 (2006).
[13] E. S. Dy and H. Kasai, J. Phys.: Condens. Matter **19**, 365240 (2007).
[14] Y. Kubota, M. C. S. Escaño, E. S. Dy, H. Nakanishi, and H. Kasai, J. Phys. Chem. **126**, 194303 (2007).
[15] M. Tsuda, E. S. Dy, and H. Kasai, J. Phys. Chem. **122**, 244719 (2005).
[16] H. Nakanishi, K. Miyamoto, M. Y. David, E. S. Dy, R. Tanaka, and H. Kasai, J. Phys.: Condens. Matter **19**, 365234 (2007).
[17] G. Kresse and J. Furthmüller, Phys. Rev. B **54**, 11169 (1996).
[18] G. Kresse and J. Furthmüller, Comput. Mater. Sci. **6**, 15 (1996).
[19] J. P. Perdew, J. A. Chevary, S. H. Vosko, K. A. Jackson, M. R. Pederson, D. J. Singh, and C. Fiolhais, Phys. Rev. B **46**, 6671 (1992).
[20] G. Kresse and D. Joubert, Phys. Rev. B **59**, 1758 (1999).
[21] H. H. Monkhorst and J. D. Pack, Phys. Rev. B **13**, 5188 (1976).
[22] C. Rovira, K. Kunc, J. Hutter, P. Ballone, and M. Parrinello, J. Phys. Chem. A **101**, 8914 (1997).
[23] G. B. Jameson, G. A. Rodley, W. T. Robinson, R. R. Gagne, C. A. Reed, and J. P. Collman, Inorg. Chem. **17**, 850 (1978).
[24] S. M. Peng and J. A. Ibers, J. Am. Chem. Soc. **98**, 8032 (1976).
[25] W. R. Scheidt and M. E. Frise, J. Am. Chem. Soc. **97**, 17 (1975).
[26] T. B. Terriberry, D. F. Cox, and D. A. Bowman, Comput. Chem. (Oxford) **26**, 313 (2002).
[27] E. S. Dy, T. A. Roman, Y. Kubota, K. Miyamoto, and H. Kasai, J. Phys.: Condens. Matter **19**, 445010 (2007).
[28] M. Tsuda and H. Kasai, Surf. Sci. **601**, 5200 (2007).